Theor Chem Acc (2003) 110:85–91
DOI 10.1007/s00214-003-0451-5

Theoretical
Chemistry Accounts

Regular article

Eliminating chaos in the Belousov–Zhabotinsky reaction by no-delay feedback and delayed feedback

Rui Zhu, Qian Shu Li

School of Chemical Engineering and Materials Science, Beijing Institute of Technology, Beijing 100081, China

Received: 4 December 2002 / Accepted: 21 April 2003 / Published online: 15 August 2003

Abstract. We present numerical simulations of the three-variable model of the Belousov–Zhabotinsky reaction developed by Gyorgyi and Field, where chaos can occur in the free-running system. As the rate of in-flow in the continuous-flow stirred-tank reactor is controlled by the concentration of one of the reactor species through a feedback loop, we find two simple ways to bring the chaotic behavior to periodic behavior. One is to modify the feedback strength without time delay in the feedback loop, and the other is to modify the delay time of the feedback at constant feedback strength. The possible mechanisms for the two ways are discussed.

Keywords: Nonlinear chemistry dynamics – Chaos control – Feedback – Delay time

Introduction

Chaotic systems, characterized by extreme sensitivity to tiny perturbations, are now known to exist widely in nature. Among them, chemical chaotic systems have attracted intensive attention because they are easily realized both in experiments and in numerical simulations and they are closely related to biological processes in life. With the development of chaos-control techniques, the control of chemical chaos has also been an important topic [1, 2, 3, 4, 5, 6, 7, 8, 9, 10, 11]. In many cases, there are two main purposes for controlling chaos. One is to eliminate chaos, and the other is to bring about a desired and well-predictable periodic behavior.

Many methods have been successfully used to control chaos [12, 13], and these methods can be mainly classified as feedback [14, 15, 16, 17, 18, 19, 20] and nonfeedback [21, 22, 23, 24, 25]. Ott–Grebogi–Yorke(OGY) [14] and Pyragas [15] are two typical feedback methods, which both utilize small perturbations to stabilize the unstable periodic orbits embedded in chaos. OGY is a discontinuous feedback method, which requires a simultaneous on-line computer analysis to determine when the feedback signal must perturb the system. OGY has been used to control chemical reactions both in simulations and in experiments [1, 2, 3]. The Pyragas method is a continuous one, which continuously applies control signals to the system by a feedback function, $F(\tau,\tau_0) = K[y(\tau-\tau_0)-y(\tau)]$, in which τ is a time-dependent measurement of the system state, τ_0 the delay time, and K the feedback strength. It has been used to stabilize the unstable periodic orbits in the Belousov–Zhabotinsky (BZ) reaction [4] and the peroxidase–oxidase reaction [5]. Recently, the self-adaptive delayed feedback controlling scheme [16] and the linear self-interacting feedback controlling scheme [18] have both been successfully used to control chaos in the BZ reaction [6, 7, 8]. In addition, the resonant chaos control method [22], which is a typical nonfeedback method, has also been proved to be useful in the control of chaos in the BZ reactions [9, 10, 11]. The resonant chaos control method is implemented by adding external periodic perturbations to the chaotic system.

Owing to the requirements for engineering, especially in communication devices, chaos controllers must be designed for fast chaotic systems [19, 20]. However, in the area of exploring some real-world chaotic systems with self-regulation behavior, such as chemical and biological systems, this requirement is not necessary since the effect of delay is often significant in such systems. Furthermore, feedback is very common in these real-world chaotic systems. Thus, exploring chaos controlling under a feedback loop with delay might be an important key to the rich phenomena of self-regulation in the real-world chaotic systems. For these reasons, in this work we use a simple continuous delayed feedback function, $F(\tau,\tau_0) = K[y(\tau-\tau_0)-y_0]$ [26, 27, 28, 29], in which the only difference from the Pyragas feedback function is that the reference concentration, y_0, is held

Correspondence to: Q.S. Li
e-mail: qsli@bit.edu.cn

constant, and we find out in a complex chemical chaotic system, i.e., the BZ reaction, whether this simple linear feedback loop could serve to bring chaos into order when the time delay exists or not. It is well known that in an automated thermostat, a simple linear system, this feedback loop can bring about a stable temperature without a time delay in the feedback and an oscillating temperature with time delay.

The BZ reaction [30, 31, 32, 33] is the best-studied example of an oscillatory chemical system, in which Ce(IV)/Ce(III) catalyses the oxidation and bromination of $CH_2(COOH)_2$ (malonic acid) by BrO_3^- in H_2SO_4. If the reaction is carried out in a continuous-flow stirred-tank reactor, the flow rate of the reactants into the tank ultimately determines the system's dynamic behavior, such as steady-steady, periodic, and chaotic behavior. As such, the flow rate is our control parameter for the system. In order to obtain good numerical simulation results, we chose the three-variable model of the BZ reaction developed by Gyorgyi and Field [34] because of its excellent accounting for rich dynamic behavior including chaos in the BZ reacting system. When the perturbation term $F(\tau,\tau_0)$ is added to the control parameter, we can modify the flow rate in two simple ways: by adjusting the feedback strength without time delay; and by adjusting the delay time at fixed feedback strength. The present work shows that the transitions from chaotic to periodic oscillations are obtained in both ways.

The model system

The chemical scheme of the BZ reaction model developed by Gyorgyi and Field is shown in Table 1. Considering the reaction rates and flow rate, the dynamic evolution equations of the studied system can be written as

$$\begin{aligned}
dX/dt &= -k_1HYX + k_2AH^2Y - 2k_3X^2 \\
&\quad + 0.5k_4A^{0.5}H^{1.5}(C-Z)X^{0.5} - 0.5k_5XZ - k_fX, \\
dY/dt &= -k_1HYX - k_2AH^2Y + \alpha k_6ZV - k_fY, \\
dZ/dt &= k_4A^{0.5}H^{1.5}(C-Z)X^{0.5} \\
&\quad - k_5XZ - \alpha k_6ZV - \beta k_7MZ - k_fZ \\
dV/dt &= 2k_1HXY + k_2AH^2Y + k_3X^2 - \alpha k_6ZV - k_fV, \quad (1)
\end{aligned}$$

where k_f is the flow rate.

Table 1. Chemical scheme of a model of the Belousov–Zhabotinsky reaction. The chemical identities of the components are $Y=Br^-$, $X=HBrO_2$, $Z=Ce(IV)$, $V=BrCH(COOH)_2$, $A=BrO_3^-$, $C=[Ce_{tot}]$, $H=H^+$, $M=CH_2(COOH)_2$. The concentration of the main reactants (A,H, and M) and the total concentration of cerium ions (C) are fixed.

Reactions	Rates(r_i)
(1) $Y+X+H \rightarrow 2V$	$r_1=k_1HYX$
(2) $Y+A+2H \rightarrow V+X$	$r_2=k_2AH^2Y$
(3) $2X \rightarrow V$	$r_3=k_3X^2$
(4) $0.5X+A+H \rightarrow X+Z$	$r_4=k_4A^{0.5}H^{1.5}(C-Z)X^{0.5}$
(5) $X+Z \rightarrow 0.5X$	$r_5=k_5XZ$
(6) $V+Z \rightarrow Y$	$r_6=\alpha k_6ZV$
(7) $Z+M \rightarrow$	$r_7=\beta k_7MZ$

If one variable changes on a faster timescale than the others in several reaction steps, a quasi-steady-state approximation could be used, i. e. d(variable)/d$t=0$. In this model, X and Y are both such kinds of variable, but we only let $dY/dt=0$ since it will make the model simpler and work better [34]. Thus, Y is eliminated in Eq. (1) by calculating $\tilde{y}$ as the root of $dY/dt=0$:

$$\tilde{y} = \left[\alpha k_6Z_0V_0zv/\left(k_1HX_0x + k_2AH^2 + k_f\right)\right]/Y_0.$$

Until now, the dimension of Eq. (1) has been decreased to 3. Then, the equations reduced are non-dimensionalized by

$$\tau \equiv t/T_0,\ x \equiv X/X_0,\ z \equiv Z/Z_0,\ v \equiv V/V_0$$

with the scaling [34]

$$T_0 = (10k_2AHC)^{-1},\ X_0 = k_2AH^2/k_5, Y_0 = 4k_2AH^2/k_5,$$
$$Z_0 = CA/(40M),\ V_0 = 4AHC/M^2.$$

Finally, the dimensionless rate equations become

$$\begin{aligned}
dx/d\tau &= T_0[-k_1HY_0x\tilde{y} + k_2AH^2Y_0/X_0\tilde{y} \\
&\quad -2K_3X_0x^2 + 0.5k_4A^{0.5}H^{1.5}X_0^{-0.5}(C-Z_0z)x^{0.5} \\
&\quad -0.5k_5Z_0xz - k_fx], \\
dz/d\tau &= T_0[k_4A^{0.5}H^{1.5}X_0^{0.5}(C/Z_0-z)x^{0.5} \\
&\quad -k_5X_0xz - \alpha k_6V_0zv - \beta k_7Mz - k_fz], \quad (2) \\
dv/d\tau &= T_0[2k_1HX_0Y_0/V_0x\tilde{y} + k_2AH^2Y_0/V_0\tilde{y} \\
&\quad +k_3X_0^2/V_0x^2 - \alpha k_6Z_0zv - k_fv].
\end{aligned}$$

See Ref. [34] for more details about the model.

Equation (2) is solved numerically using the Gear method. The parameters used in Eq. (2) are listed in Table 2. The bifurcation diagram for Eq. (2) with the variation of k_f is shown in Fig. 1 and agrees with the result of Gyorgyi and Field [34]. Steady states appear at $k_f \le 2.350\times10^{-4}$ s^{-1}(not shown in Fig. 1), and small-amplitude, sinusoidal period-1 oscillations develop as k_f is increased. The sequence of period-doubling bifurcations follows and results in chaos at $k_f \approx 3.230\times10^{-4}$ s^{-1}. Several other periodic and chaotic windows appear as k_f is increased to 4.450×10^{-4} s^{-1}, above which the regular period-1 oscillation appears again. For the present study, we focus on the strange attractor at $k_{f_0} = 3.400\times10^{-4}$ s^{-1}, which has been characterized by

Table 2. Parameters used in Eq. (2) [34]

Rate constants (k_i) for reactions 1–7	Other parameters
$k_1=4.0\times10^6$ M^{-2} s^{-1}	$A=0.1$ M,$M=0.25$ M,
$k_2=2.0$ M^{-3} s^{-1}	$H=0.26$ M,$C=8.33\times10^{-4}$ M,
$k_3=3.0\times10^3$ M^{-1} s^{-1}	$\alpha=666.7$, $\beta=0.3478$
$k_4=55.2$ M$^{-2.5}$ s^{-1}	
$k_5=7.0\times10^3$ M^{-1} s^{-1}	
$k_6=0.09$ M^{-1} s^{-1}	
$k_7=0.23$ M^{-1} s^{-1}	

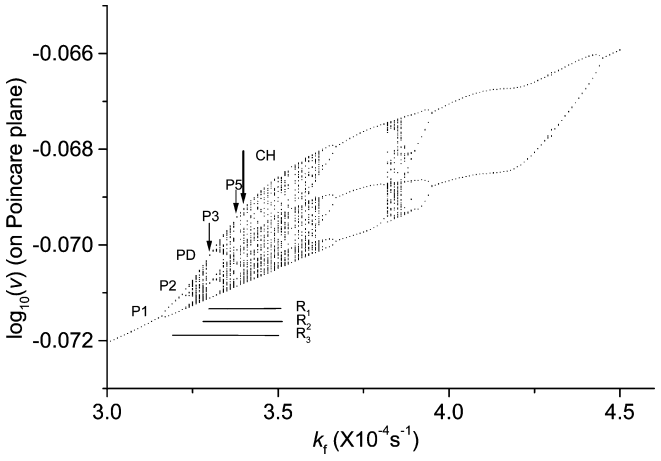

Fig. 1. Bifurcation diagram obtained from simulations based on Eq. (2) by gradually increasing the flow rate, k_f. The conditions for these simulations are listed in Table 2. Periodic behavior is indicated when only a few intersections are visible at a particular k_f, whereas many intersections indicate chaos. *PD* sequence of period-doubling bifurcation, *CH* chaos regime, *P2* period-2 oscillation, *P3* period-3 oscillation, *P5* period-5 oscillation. R_1, R_2, and R_3 denote the variation ranges of k_f at $K=4.54\times10^{-6}$, 6.05×10^{-6}, and 1.06×10^{-5} s^{-1} in Eq. (3) without time delay, respectively. The *thick arrow* indicates the chaos at $k_f=3.400\times10^{-4}$ s^{-1} studied in this work

the Poincare surface of section, the frequency spectrum, and the 1D return map (not shown here), and calculate the flow rate, k_f, in Eq. (2) with the following formula

$$k_f = k_{f_0} + F(\tau, \tau_0) = k_{f_0} + K[z(\tau - \tau_0) - z_0], \qquad (3)$$

in which k_{f_0} is a constant component, K the feedback strength, z $(\tau-\tau_0)$ the value of z after a delay time of τ_0, and z_0 the constant reference value. We take z_0 to be 4.50 throughout this work, which is about the middle value between the maximum and minimum of the oscillations for the free-running oscillator at $k_{f_0} = 3.400 \times 10^{-4}$ s^{-1}.

Eliminating chaos

Case 1: Modifying the feedback strength without time delay

In this case, there is no time delay in Eq. (3). We increase K from 7.56×10^{-7} s^{-1} to 1.51×10^{-5} s^{-1} in steps of 7.56×10^{-7} s^{-1}. It is found that when $K=4.54\times10^{-6}$–6.05×10^{-6} s^{-1} and 1.06×10^{-5}–1.51×10^{-5} s^{-1}, the transitions from chaotic to periodical oscillations occur. The former range of K is called region 1, and the latter is called region 2. The transitions for regions 1 and 2 are illustrated in Fig. 2a and b, respectively. In region 1, only period-3 oscillations are obtained, while in region 2 period-4 and period-2 oscillations are both obtained. A point of interest is that the shapes and amplitudes for the periodic oscillations obtained in region 1 vary a little, while they change much in region 2, in particular, the amplitudes have a decreasing trend with the increment

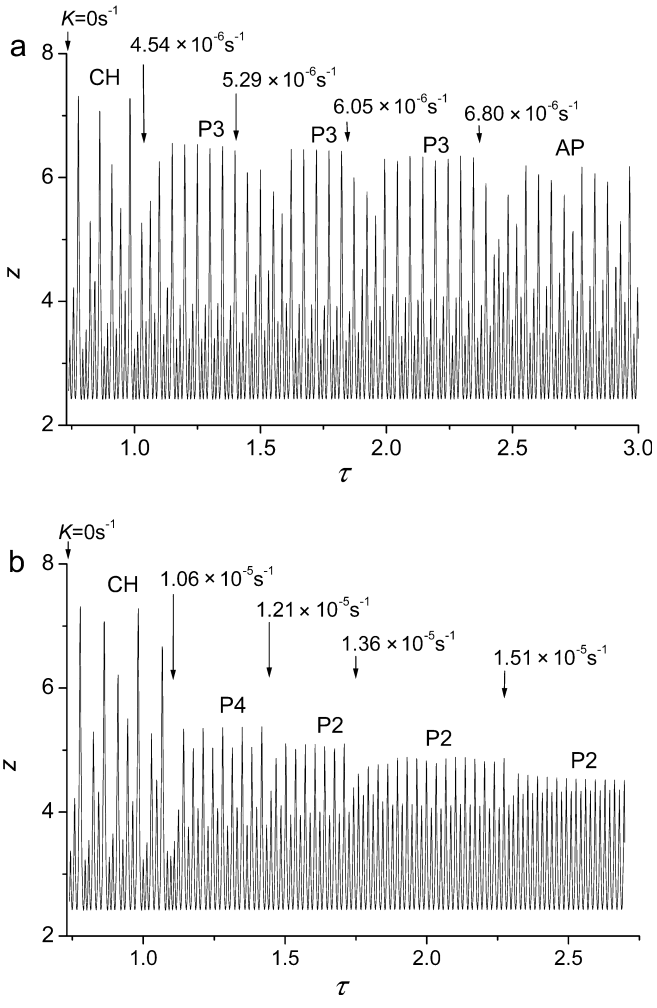

Fig. 2a, b. Reduced concentration of Ce(IV), z, as a function of reduced time, τ, obtained from Eq. (2) for the transitions from chaos to periodic oscillations when the system has no-delay feedback. The *arrows* indicate when the control feedback is switched on, and the *numbers* on the arrows show the values of the feedback strength, K, applied. *CH* chaotic state, *P* periodic state, *AP* aperiodic state. **a** Values of K between 4.54×10^{-6} and 6.05×10^{-6} s^{-1}, and **b** values of K between 1.06×10^{-5} and 1.51×10^{-5} s^{-1} are illustrated to serve to eliminate chaos

of K. Note that, in Fig. 2a, after $K=6.80\times10^{-6}$ s^{-1} is switched on, the subsequent oscillations are marked by AP, i.e., aperiodic oscillation, since the original chaos may be destroyed by the applied perturbation.

Case 2: Modifying the delay time with constant feedback strength

By the previous means, only a small range of values between $K=7.56\times10^{-7}$ and 1.06×10^{-5} s^{-1} can serve to eliminate chaos. The question then becomes how to use the other values to eliminate the chaos. Consider now that the time delay exists in Eq. (3) and modify the delay time with K fixed to be a value between 7.56×10^{-7} and 1.06×10^{-5} s^{-1} except for the small range 4.54×10^{-6}–

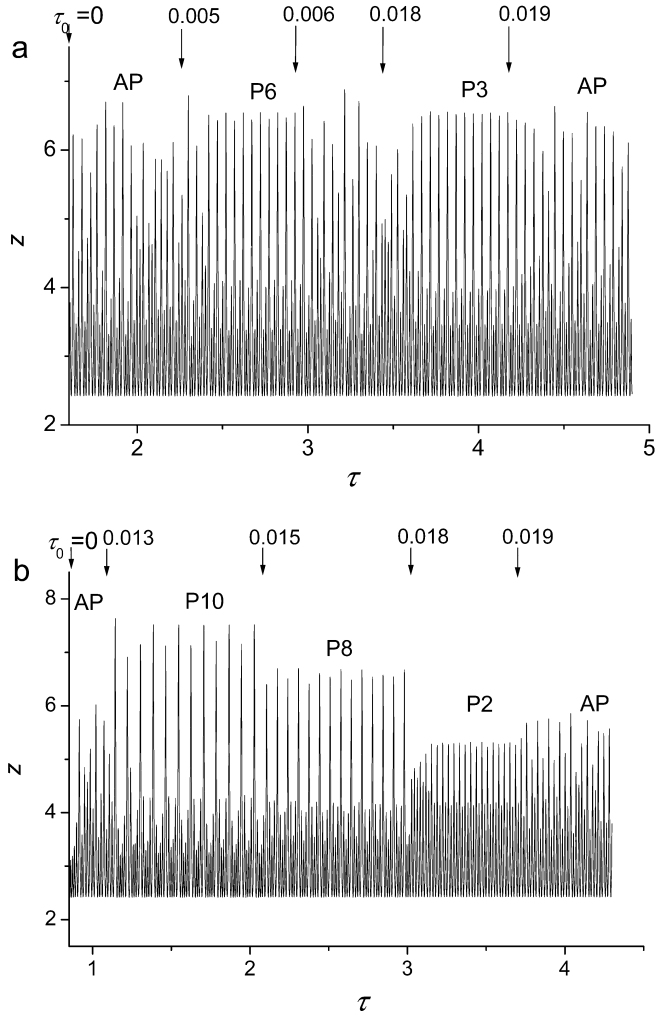

Fig. 3a, b. Reduced concentration of Ce(IV) z as a function of reduced time τ obtained from Eq. (2) for the transitions from chaos to periodic oscillation by adjusting the delay time, τ_0, with fixed feedback strength in Eq. (3). **a** $K=3.78\times10^{-6}$ s^{-1}. **b** $K=7.56\times10^{-6}$ s^{-1}. Notations are the same as those in Fig. 2

6.05×10^{-6} s^{-1}. It is found that for each value of K that we choose there exist delay times that can turn chaos into periodicity. It is more interesting that when K is fixed to a value between 7.56×10^{-7} and 4.54×10^{-6} s^{-1}, the delay times for transitions are almost symmetric, i.e., there exist two sets of delay time. However, when K is increased to a value between $6.05\times10^{-6}$and 1.06×10^{-5}s^{-1}, this symmetry is destroyed. The former range of K, i.e., 7.56×10^{-7}–4.54×10^{-6} s^{-1}, is called region 3; the latter range of K, i.e., 6.05×10^{-6}–1.06×10^{-5} s^{-1}, is called region 4. We take two values of K as examples for the cases in regions 3 and 4, respectively. The transitions at $K=3.78\times10^{-6}$ s^{-1} with adjustment of the delay time are shown in Fig. 3a. It indicates that there are two sets of delay time and that they are around $\tau_0=0.005$ and 0.018, respectively. The transitions at $K=7.56\times10^{-6}$ s^{-1} are shown in Fig. 3b, but only one big set of delay time, i.e., $\tau_0=0.013$–0.018, is found. A common feature as shown in case 1 is that the transformed periodic oscillations in region 3 change a little with τ_0, while those in region 4 change significantly. It seems, however, that richer periodic oscillations could be obtained than those by no-delay feedback.

One may wonder why the integration time needed for determining the dynamic behavior of the system seems very short in Figs. 2 and 3. In fact, these figures just illustrate the results which are obtained in the long simulations. As shown in Figs. 2 and 3, the regular oscillations are stabilized soon after the feedback is switched on or changed, indicating that the system studied responds rapidly to the perturbations.

Discussions

For case 1 we analyze the variation ranges of k_f as it is perturbed according to Eq. (3) at the values of K ranging from 7.56×10^{-7} to 1.51×10^{-5} s^{-1}, and compare them with the bifurcation diagram of the system without perturbations. It is found that the transitions from chaos to periodicity in case 1 seem to be attributed to the periodic windows in the bifurcation diagram. In Fig. 1 we plot the variation ranges of k_f at $K=4.54\times10^{-6}$, 6.05×10^{-6}, and 1.06×10^{-5}s^{-1}, which are denoted by R_1, R_2, and R_3 respectively. When $K<4.54\times10^{-6}$ s^{-1}, the minima of the k_f variations, called R_m, are almost in the chaotic window, and transitions from chaos to periodicity are not found. When K increases to a value between 4.54×10^{-6} and 6.05×10^{-6} s^{-1}, R_m crosses a little the period-3 window, and transitions from chaos to periodicity occur. When K increases from 6.05×10^{-6} s^{-1}, R_m goes far beyond the period-3 window and walks deep into another chaotic region, and transitions from chaos to periodicity disappear. Until $K\geq1.06\times10^{-5}$ s^{-1}, as R_m walks deep into the periodic window, transitions from chaos to periodicity reappear. From the previous analysis, we suppose that whether the transitions occur or not depends on where the minima of the k_f variations lie in the bifurcation diagram. It is understandable if we note that the minimal part of the k_f variations just corresponds to the small-amplitude oscillations of z. And such small-amplitude oscillations can be considered as the transitional states that jump to big oscillations. These transitional states determine when the next big oscillation occurs. Therefore, as long as the values of k_f corresponding to transitional states lie sufficiently in periodic windows, the periodic windows will probably like "traps" pull the chaos into them.

If carefully seen, the bifurcation diagram in Fig. 1 has a much smaller window for period-5, which is near the chaotic state at $k_{f_0}=3.400\times10^{-4}$ s^{-1}. On the basis of the previous analysis, besides regions 1 and 2, there should exist a third set of delay time corresponding to the period-5 window for transitions from chaos to periodicity. So we decreased the increment of K in case 1, and we found this small set of delay time, i.e., $K=9.83\times10^{-7}$–1.13×10^{-6} s^{-1} (region 5). For an illustration of the transitions see Fig. 4. It is interesting

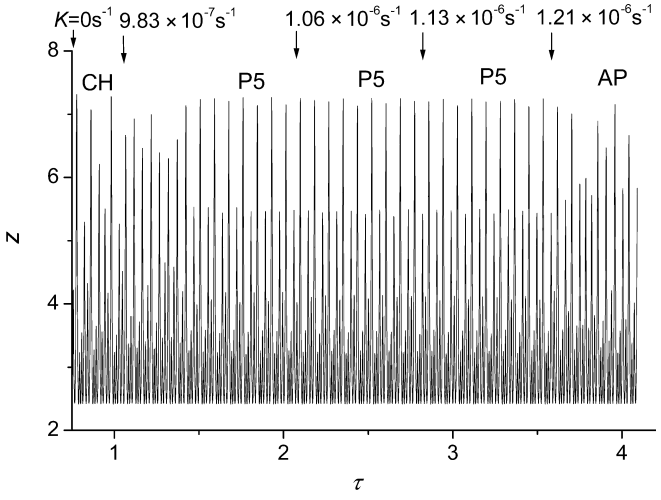

Fig. 4. Same as in Fig. 2 except that the values of K between 9.83×10^{-7} and 1.13×10^{-6} s^{-1} are illustrated to serve to control chaos

that only period-5 oscillations are obtained. Since the magnitudes of K are quite small for the cases in region 5, the period-5 oscillations obtained vary less than those in regions 1 and 2. On the basis of these facts, we believe that the no-delay feedback method for case 1 depends strongly on the periodic windows in the bifurcation diagram. Further clear proof supporting this conclusion is that the periodic oscillations obtained in regions 5, 1, and 2 include period-5 (Fig. 4), period-3 (Fig. 2a), period-4 (the first stabilized periodic oscillations in Fig. 2b), and period-2 (the last three stabilized periodic oscillations in Fig. 2b) oscillations. They respectively correspond to the windows of period-5, period-3, period-4, and period-2 in the bifurcation diagram (Fig. 1). As mentioned previously, these periodic windows like traps pull the chaos into them.

It should be noted that the periodic oscillations obtained in this way are not the unstable periodic orbits embedded in the original chaotic attractor because k_f had a wide range of variation in the control process. This is in accord with the results which were obtained by the linear feedback loop through the function, $k_f = k_{f_0} \times [1 + C \times z(\tau)] + R$, where C was called the self-interacting strength and R the regulator by Song et al. [6, 7, 8]. In fact, this feedback function is the same as the no-delay feedback function used here; their C corresponds to our K, and their R to our $z(\tau_0)$. Song et al. focused on adjusting the parameter C with R being zero or positive. Thus, in their control process only positive or only negative feedback can exist depending on whether C is positive or negative. By using the scheme, they experimentally obtained period-1 and period-2 oscillations in the ordinary BZ chaos [7] and only period-1 in the new BZ chaos they discovered [8]. Also, they numerically got the steady state, period-1, period-2, period-3, and period-4 in a four-variable BZ chaotic model [6]. In the present studies, K remains positive, and $z(\tau_0)$ is set to the middle value between the maximum and the minimum of the oscillations, so positive and negative feedback may alternate in the control process. The periodic oscillations obtained here include period-2, period-3, period-4, and period-5.

The mechanism for case 1 does not seem to account for the transitions in case 2 with time delay in the feedback, especially as K is in region 3, where no part of the variations of k_f lies in periodic windows. By comparisons of the time series of z with those of k_f for the controlled cases in region 3, we find that one set of delay time causes the first valley following the biggest peak in the periodic oscillations of z corresponding to the right side of the biggest peak of k_f, and the other set to the left side, indicating symmetry. An example of such a case at $K = 3.78\times10^{-6}$ s^{-1} with $\tau_0 = 0.005$ and 0.018 is shown in Fig. 5. Keeping in mind the analysis mentioned for case 1, we propose that among the small-amplitude oscillations that determine the whole oscillations, the first valleys following the biggest peaks could be the most important. So, we can describe a possible mechanism for case 2 as follows. The controlled system utilizes by the time delay the state information of the biggest peak to make the first valley following this peak correspond to suitable values of k_f, then under this condition periodic oscillations become stable. The fact

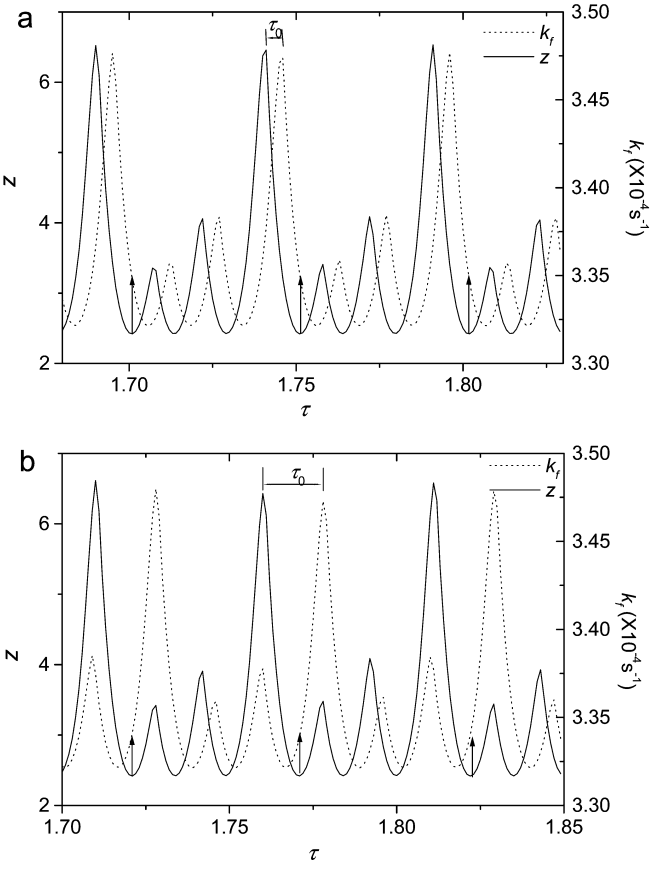

Fig. 5a, b. Time traces for z and k_f for the periodic oscillations obtained from the case of $K = 3.78\times10^{-6}$ s^{-1} in Fig. 3. **a** $\tau_0 = 0.005$. **b** $\tau_0 = 0.018$. The *arrows* indicate the values of k_f corresponding to the first valley following the biggest peak in the oscillations of z

that the symmetry of the set of the delay time is destroyed for the controlled cases in region 4 may be caused by the big periodic windows involved. Though a possible mechanism for case 2 is given here, some problems, such as why different feedback strengths lead to different ranges of delay time for controlling chaos and why different delay times may produce different forms of periodic oscillation, are still unsolved. Thus, more detailed investigations are needed to account for these phenomena. Like case 1, the periodic oscillations obtained in case 2 are not the unstable periodic orbits embedded in the original chaotic attractor, because the values of the feedback function do not tend to zero.

It should be noted that the mechanism for case 2 is different from that of the Pyragas delayed feedback method. The control signals generated by the Pyragas feedback function $K[y(\tau-\tau_0)-y(\tau)]$ could tend to zero when τ_0 is chosen to be equal to the period of an unstable orbit in a strange attractor, while those in case 2, as mentioned earlier, have comparatively large amplitudes as chaos is controlled. However, the mechanism for case 2 may be related to those for external periodic perturbation methods [22], since the control signals generated by the feedback loop in case 2 are periodic when chaos is controlled. The key point here is that the controlled system itself generates such periodic signals through a feedback loop with time delay.

Comparing cases 1 and 2, we think that the delayed feedback method used in case 2 is more useful than the no-delay one used in case 1, because it is not periodic-window dependent. We also use the delayed feedback method to the chaos at other values of k_f in the bifurcation diagram in Fig. 1, and the transitions from chaos to order are all successfully obtained. On the other hand, the implications of the present results to real-world chaotic systems, as stated in the Introduction, are obvious, i.e., the complex chaotic system studied here has the ability to self-regulate through a simple feedback loop. In addition, the results have special implications in signal processing in biological systems. Recent work has indicated that feedback interactions could impart precision, robustness, and versatility to intercellular signals during animal development [35]. Besides these advantages, we suppose that just like the two cases in this work a biological unit may by a feedback loop provide different signals, such as chaotic, aperiodic, and different-period periodic signals, to other biological units, causing different biological effects.

Conclusion

Among the continuous-feedback methods used for controlling chaos, we used a method whose feedback function has the form $K[y(t-\tau)-y_0]$. The main new point in this work is that this simple linear feedback loop can in two ways serve to eliminate the chaos in a complex BZ reaction model, i.e., to turn chaotic into periodic oscillations. One way is to modify the feedback strength K to proper values as the delay time τ equals zero, and the other is to modify the delay time to adequate values at fixed feedback strength. The two means imply, respectively, a mechanism of self-regulation for the BZ reaction. On the other hand, the feedback method used here, where the reference value is a constant in time, needs further testing in other chaotic systems. Its characteristics and application range should be investigated in detail.

From the experimental point of view, the model used in this study is realistic enough to reproduce the experimentally observed behavior of the BZ reaction in a continuous stirred tank reactor and an experimental realization of the two methods used in this work is simple. Thus, it would be interesting if our results can be tested in real experiments.

Acknowledgments. The authors gratefully thank Shawn T. Brown for valuable comments. This work is supported by the National Natural Science Foundation of China.

References

1. Peng B, Petrov V, Showalter K (1991) J Phys Chem 95:4957
2. Petrov V, Peng B, Showalter K (1992) J Chem Phys 96:7506
3. Petrov V, Gaspar V, Masere J, Showalter K (1993) Nature 361:240
4. Schneider FW, Blittersdorf R, Forster A, Hauck T, Lebender D, Muller J (1993) J Phys Chem 97:12244
5. Lekebusch A, Forster A, Schneider FW (1995) J Phys Chem 99:681
6. Song H, Li Y-N, Chen L, Cai Z-S, Li Y-J, Hou Z, Zhao X-Z (1999) Phys Chem Chem Phys 1:813
7. Song H, Li Y-N, Chen L, Cai Z-S, Li Y-J, Hou Z, Wu B-X, Zhao X-Z (1999) Acta Chim Sin Chin Ed 57:1047
8. Li Y-N, Song H, Chen L, Cai Z-S, Li Y-J, Hou Z, Wei Q-L, Wu B-X, Zhao X-Z (2001) Can J Chem 79:29
9. Kraus M, Muller J, Lebender D, Schneider FW (1996) Chem Phys Lett 260:51
10. Guderian A, Munster AF, Kraus M, Schneider FW (1998) J Phys Chem A 102:5059
11. Guderian A, Munster AF, Jinguji M, Kraus M, Schneider FWV (1999) Chem Phys Lett 312:440
12. Shinbrot T, Grebogi C, Ott E, Yorke JA (1993) Nature 363:411
13. Boccaletti S, Grebogi C, Lai Y-Ci, Mancini H, Maza D (2000) Phys Rep 329:103
14. Ott E, Grebogi C, Yorke JA (1990) Phys Rev Lett 64:1196
15. Pyragas K (1992) Phys Lett A 170:421
16. Kittel A, Parisi J, Pyragas K (1995) Phys Lett A 198:433
17. Pyragas K (1995) Phys Lett A 206:323
18. Chen C-C, Tsai C-H, Fu C-C (1994) Phys Lett A 194:265
19. Myneni K, Barr TA, Corron NJ, Pethel SD (1999) Phys Rev Lett 83:2175
20. Corron NJ, Pethel SD, Hopper BA (2000) Phys Rev Lett 84:3835
21. Lima R, Pettini M (1990) Phys Rev A 41:726
22. Braiman Y, Goldhirsch I (1991) Phys Rev Lett 66:2545
23. Chang K, Kodogeorgiou A, Hubler AW, Jackson EA (1991) Physica D 51:99
24. Liu Y, Leite JRR (1994) Phys Lett A 185:35
25. Mettin R, Kurz T (1995) Phys Lett A 206:331
26. Weiner J, Schneider FW, Bar-Eli K (1989) J Phys Chem 93:2704
27. Weiner J, Holz R, Schneider FW, Bar-Eli K (1992) J Phys Chem 96:8915
28. Roesky PW, Doumbouya SI, Schneider FW (1993) J Phys Chem 97:398

29. Zeyer KP, Holz R, Schneider FW (1993) Ber Bunsenges Phys Chem 97:1112
30. Field RJ, Burger M (1985) Oscillations and travelling waves in chemical systems. Wiley, New York
31. Field RJ, Koros RJ, Noyes RM (1972) J Am Chem Soc 94:8649
32. Belousov BP (1958) Sb Ref Radiats Med Medgiz Moscow 145–147
33. Zhabotinsky AM (1964) Biofizika 9:306
34. Gyorgyi L, Field RJ (1992) Nature 355:808, and references therein
35. Freeman M (2000) Nature 406:313